nature cell biology

A bistable Rb–E2F switch underlies the restriction point

Guang Yao[1,2], Tae Jun Lee[3], Seiichi Mori[1,2], Joseph R. Nevins[1,2,4], and Lingchong You[1,3,4]

The restriction point (R-point) marks the critical event when a mammalian cell commits to proliferation and becomes independent of growth stimulation. It is fundamental for normal differentiation and tissue homeostasis, and seems to be dysregulated in virtually all cancers[1,2]. Although the R-point has been linked to various activities involved in the regulation of G1–S transition of the mammalian cell cycle[2–6], the underlying mechanism remains unclear[1,7]. Using single-cell measurements, we show here that the Rb–E2F pathway functions as a bistable switch to convert graded serum inputs into all-or-none E2F responses. Once turned ON by sufficient serum stimulation, E2F can memorize and maintain this ON state independently of continuous serum stimulation. We further show that, at critical concentrations and duration of serum stimulation, bistable E2F activation correlates directly with the ability of a cell to traverse the R-point.

The concept of an R-point[8] suggests that removal of growth stimuli before this point in the G1 phase of the cell cycle shifts a cell back to quiescence; after that, the cell cycle progresses independently of growth stimulation[8,9]. The key characteristic of the R-point is two-fold: first, an initial high threshold on growth stimulation is set to ensure prerequisites for fully executing proliferation are fulfilled; second, a low-maintenance mechanism ensures that the cell cycle is completed once initiated, even in the absence of sustained growth signals. This 'high-threshold, low-maintenance' nature of the R-point is reminiscent of a bistable switch mechanism recently identified in several decision-making processes, including oocyte maturation and regulation of mitosis in frogs[10,11], nutrient utilization in bacteria[12] and the mating response in yeasts[13]. Control of the R-point in mammalian cells by a bistable mechanism was suggested by mathematical modelling analyses[14–18], but has not been demonstrated experimentally.

Here we probe the bistable nature of the Rb–E2F pathway and its control of the R-point by examining the kinetic properties of E2F activation in response to serum stimulation. E2F is a transcriptional factor that can activate genes encoding proteins involved in DNA replication and cell-cycle progression[3–5], and is essential in the regulation of cell proliferation[19,20]. Topologically, E2F functions as the output of the Rb–E2F signalling pathway and is involved in multiple positive-feedback loops (Fig. 1a). In quiescent cells, E2F is bound to and repressed by Rb. With sufficient growth stimulation, phosphorylation by Myc-induced cyclin D (CycD)–Cdk4,6 removes Rb repression; Myc also induces E2F transcription[21]. Subsequently, E2F activates the transcription of CycE, which forms a complex with Cdk2 to further remove Rb repression by phosphorylation, establishing a positive-feedback loop. E2F also activates its own transcription, constituting another positive-feedback loop. Regulation by positive feedback is a hallmark of a bistable switch[22,23]. Together, the two positive-feedback circuits described above and others not shown for simplicity (for example, that involving mutual inhibition between CycE–Cdk2 and $p27^{Kip1}$) suggests the potential for the Rb–E2F pathway to generate bistability.

To analyse the dynamics of the Rb–E2F pathway, we first constructed a simple mathematical model composed of a system of coupled ordinary differential equations (Supplementary Information, Tables S1–3). To reduce complexity and generate experimentally tractable predictions, this model was restricted to interactions involved in the cell cycle entry-phase (Fig. 1a) and we chose to ignore downstream oscillation events. It was not intended to account for all aspects of the intricate regulation in the G1–S transition of the mammalian cell cycle. Rather, this simplified model was useful as framework for analysing the qualitative properties of the underlying control system.

Our model suggests that the Rb–E2F pathway may indeed generate bistability in E2F activation. It predicts that the serum concentration must reach a critical threshold (approximately 1% in this example, Fig. 1b) to activate E2F from its previous OFF state. Once turned ON, however, E2F can maintain this state even when the serum concentration falls below the initial threshold. Within a certain range of serum concentration (0.2–1%), the steady-state E2F level is bistable and can be either ON or OFF, depending on its previous state. In comparison, circuit components not regulated by positive-feedback (for example, CycD) are likely to be monostable, with their steady-state levels dependent only on the final serum concentration (Fig. 1c).

To test the bistable E2F accumulation, we used a destabilized green fluorescent protein (d2GFP) reporter to probe the E2F transcriptional activity at the single-cell level. This d2GFP reporter, under the control of a cloned E2F promoter, was first stably integrated into the chromosome

[1]Institute for Genome Sciences and Policy, Duke University, Durham, NC 27708, USA. [2]Department of Molecular Genetics and Microbiology, Duke University Medical Center, Durham, NC 27710, USA. [3]Department of Biomedical Engineering, Duke University, Durham, NC 27708, USA.
[4]Correspondence should be addressed to: L.Y. or J.R.N. (e-mail: you@duke.edu; j.nevins@duke.edu)

Received 11 November 2007; accepted 21 January 2008; published online 23 March 2008; DOI: 10.1038/ncb1711

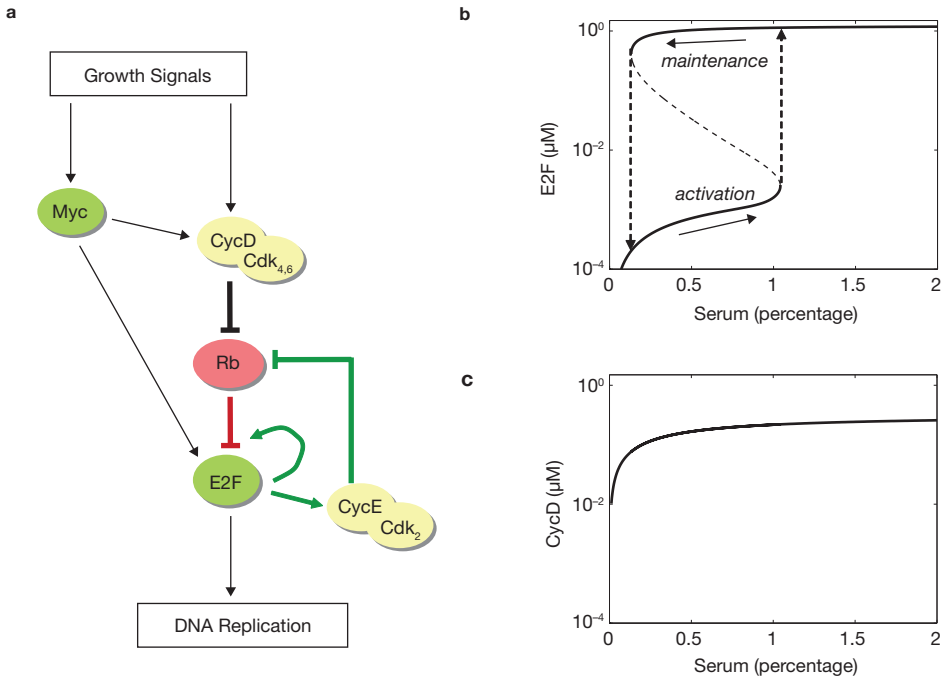

Figure 1 Simplified model of the bistable Rb–E2F switch. (**a**) The Rb–E2F circuit. E2F represents all E2F activators (E2F1, E2F2 and E2F3a). Rb represents all pocket proteins (Rb, p130 and p107). (**b**, **c**) Simulated steady-state concentration-dependent responses of E2F and CycD to serum stimulation.

of rat embryonic fibroblasts (REF52). We further established single-cell clones, each bearing the same E2F–d2GFP integration background, and also constructed a CycD–d2GFP reporter system in parallel to function as a negative control (Supplementary Information, Fig. S1). Both d2GFP reporter systems showed serum responses that were comparable to their endogenous counterparts, in their concentration-dependent and time-course characteristics (Fig. 2d, e, Supplementary Information, Fig. S1).

We found that E2F accumulation had a bimodal distribution in a clonal cell population, a hallmark of a bistable system[12,24]. To test the model-predicted, steady-state characteristic of E2F activation, we stimulated quiescent cells with serum at different concentrations and measured E2F–d2GFP endpoint levels (see Methods). Figure 2a shows the E2F response to increasing concentrations of serum in four independent cell clones assayed in parallel. At intermediate serum concentrations (in particular, 0.5–1%, although the exact distribution pattern varied between cell clones0, E2F–d2GFP distributions were ubiquitously bimodal. This bimodality suggests that the intrinsic ultrasensitive E2F activation responds to a specific range of serum stimulation. Outside this range, when serum concentrations were sufficiently low (<0.2%) or sufficiently high (>2%), the E2F–d2GFP levels were unimodally OFF or ON in all cell clones.

E2F bimodality shows 'all-or-none' switching behaviour in its activation. That is, although individual cells responded to different strengths of serum stimulation, in one given cell, the steady-state level of E2F expression was either OFF or ON. Supporting this notion, increasing the serum concentration caused a gradual decrease in the number of cells with E2F–d2GFP levels at the OFF state (Fig. 2a, left peak) and a corresponding increase in the number of cells with E2F–d2GFP level at the ON state (Fig. 2a, right peak). Few cells had E2F–d2GFP levels at intermediate states. In comparison, the expression of CycD–d2GFP was always unimodal under the same test conditions. Its steady-state level gradually increased as a function of serum concentration, without a clearly differentiated OFF or ON state (Fig. 2b). Therefore, it appears that the conversion from graded serum input into binary cellular responses is mediated by network modules topologically located between CycD and E2F (Fig. 1a).

The bimodal E2F response in clonal populations probably resulted from the interplay between bistability in E2F activation (Fig. 1b) and stochasticity in signalling dynamics. Such stochastic effects (or cellular noise) could arise from heterogeneity in the extracellular environment, small numbers of interacting molecules or perturbations by unaccounted-for cellular processes[25–28]. In contrast, CycD expression remained unimodal under cellular noise, which probably reflects its monostable nature (Fig. 1c). To explore the degree of stochasticity affecting E2F bimodal responses, we measured E2F responses in a same cell clone (no. 23). Measurements were repeated six times. Each time, we observed distinct bimodality in E2F responses, yet E2F distributions around the switching-point (between 0.5%–1% serum) varied substantially from experiment to experiment (Supplementary Information, Fig. S3). The stochasticity evident in E2F and CycD responses underscores the importance to probe bistability at the single-cell level. In particular, cell-to-cell variation will cause a smoothed-out transition between the OFF and ON states in population-averaged measurements (for example, real-time RT-PCR; Fig. 2d, e), a phenomenon described previously (for example, in the lactose utilization network of *Escherichia coli*)[12]. This averaging effect would obscure the ultrasensitive E2F response in individual cells (Figs 1b, 2a), as well as the distinct features of E2F and CycD activation observed with single-cell resolution.

We also found that E2F accumulation showed marked history-dependence (hysteresis), another characteristic of a bistable switch. History-dependence is a property of a system whose output reacts with a delay to the input change, or does not return completely to its original level. This property is often examined by first inducing the output to a sufficiently high steady state with a strong input, and then reducing the

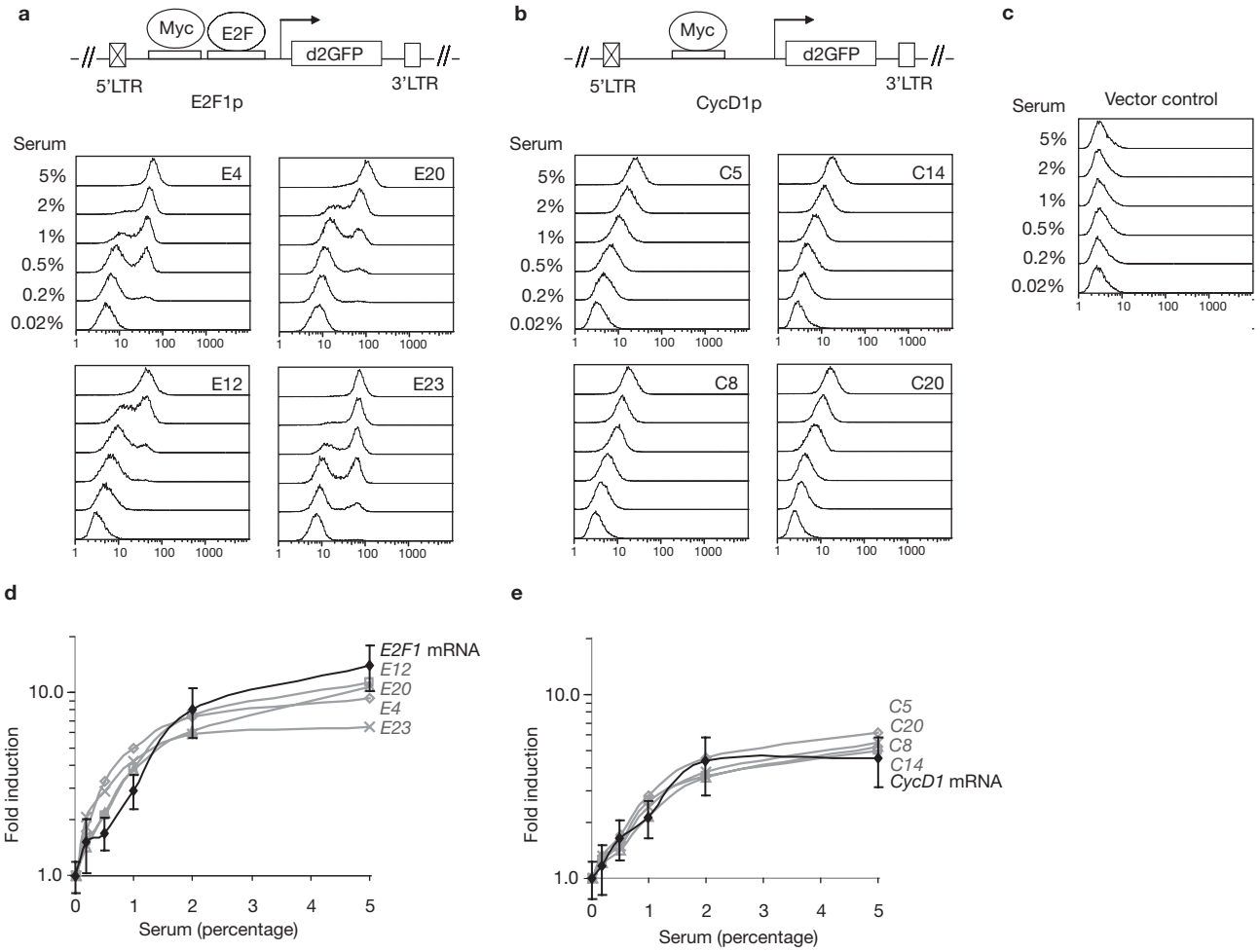

Figure 2 Bimodal E2F expression in cultured mammalian cells. (**a**–**c**) Cells were serum-starved (0.02% BGS) for 1 day and subsequently stimulated with BGS at the indicated concentrations. Hydroxyurea was applied to synchronize cells at G1–S at the time of assay (24 h after serum-stimulation) and it did not seem to affect the endpoint responses of E2F or CycD (Supplementary Information, Fig. S2). Each histogram represents the d2GFP distribution from approximately 10,000 cells. Responses of E2F (**a**, lower panels) and CycD (**b**, lower panels) from four independent clones (Supplementary Information, Fig. 1) and an empty-vector control (**c**) to different concentrations of serum are shown. E2F–d2GFP (**a**, upper panel) and CycD–d2GFP (**b**, upper panel) reporter constructs are shown. (**d**, **e**) Comparison between population-averaged d2GFP reporter levels in each cell clone in **a** and **b** (normalized to the autofluorescent background in **c**) and the endogenous E2F1 and CycD1 mRNA levels in REF52 cells at corresponding treatment conditions, measured by real-time RT-PCR (mean ± s. e. m., calculated from three replicates normalized to a loading control).

input to low levels to analyse the new output steady states. In cell-cycle experiments, however, the short interval between cell divisions and the complex oscillation events do not allow measurement of output change between established steady states.

We probed the history-dependence of the Rb–E2F gene network by studying its influence on E2F accumulation with a serum pulse. Our model predicts that when quiescent cells are treated with serum at a low concentration, inadequate to activate proliferation (0.3%, Fig. 3b), the E2F level will remain in its OFF state; following a strong serum pulse (sufficient to activate the Rb–E2F bistable switch), the final E2F level in the same low-serum concentration (0.3%) will reach and stay at the ON state (Fig. 3a, b). This distinction in E2F activation, responding to the same final serum input, provides proof of its bistability. In comparison, regardless of the pulse-stimulation history, the final CycD level will be at the same state (Fig. 3b).

The predicted E2F history-dependence was indeed observed in our experiments. In particular, we compared E2F responses at a range of final serum inputs, with or without an initial strong serum pulse (20% for 5 h). At final serum concentrations between 0.2% and 1%, E2F–d2GFP endpoint levels in most cells were found in the OFF state without the pulse stimulation (Fig. 3c, red curves), whereas they were in the ON state with the pulse stimulation (Fig. 3c, green curves). In contrast, the presence or absence of the initial serum pulse did not have a significant effect on the endpoint levels of the CycD–d2GFP control (Fig. 3c), consistent with the reported rapid turnover of CycD expression after withdrawal of growth factors[29]. As the same d2GFP reporter was used in both cases, the history-dependence of E2F, compared with CycD, probably reflects the inherent distinction in their transcription regulation by the underlying gene network (Fig. 1a). Consistently, the E2F history-dependence was observed at different measurement times with different synchronization methods (Supplementary Information, Fig. S4).

Furthermore, we found that the bistable E2F accumulation was directly correlated with the ability of a cell to traverse the R-point in response to graded serum inputs. Consistent with the R-point

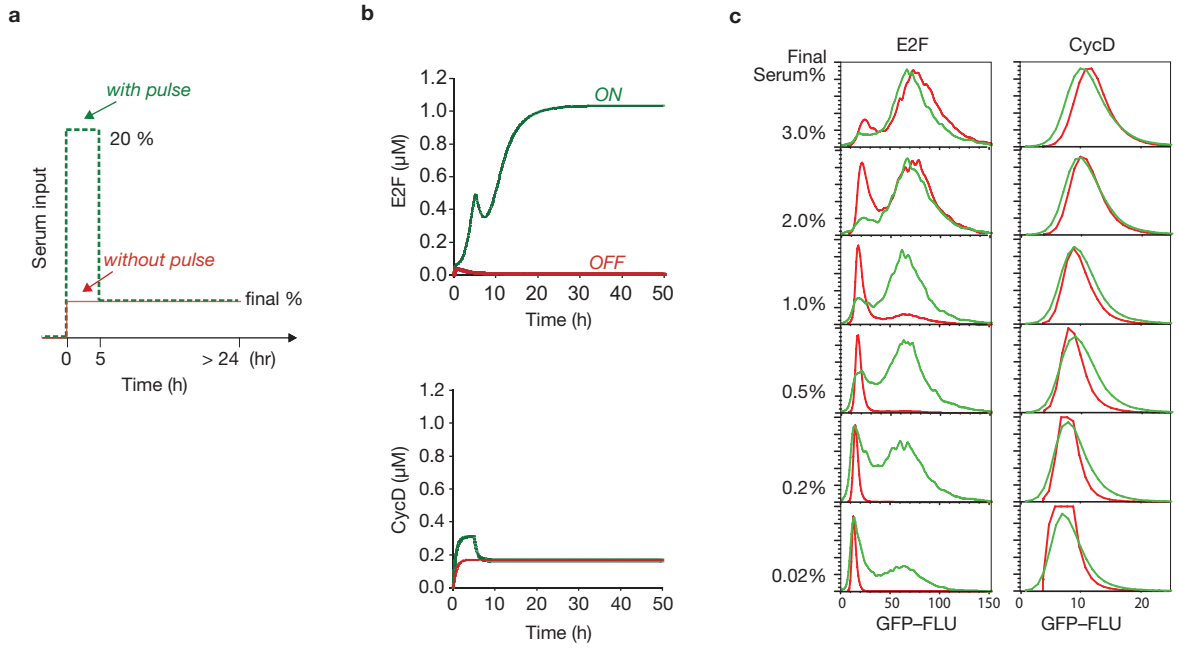

Figure 3 History-dependence of E2F. (**a**–**c**) Red curves, without serum pulse; green curves, with pulse. (**a**) Serum-pulse stimulation-protocol. At time 0, cells were serum-starved and quiescent. (**b**) Model prediction of E2F and CycD responses to serum pulse (final concentration was 0.3%). (**c**) E2F–d2GFP and CycD–d2GFP responses to serum pulse. Final serum concentrations were as indicated. Each histogram represents d2GFP distribution from approximately 10,000 cells (E2F clone no. 23, CycD clone no. 5, Supplementary Information, Fig. S1) after baseline correction (Supplementary Information, Fig. S5). Cells were synchronized at G1–S by hydroxyurea at the time of assay (24 h after serum-stimulation).

concept, following an initial strong serum pulse (20% for 5 h in this case), most cells were able to enter the cell cycle at a final serum concentration as low as 0.2% (Fig. 4a, green arrow), as indicated by their incorporation of 5-bromodeoxyuridine (BrdU; Fig. 4a, magenta dots) during DNA replication at the S-phase. In comparison, without such pulse-stimulation, most cells remained quiescent (until treated with serum at concentrations greater than 1%; Fig. 4a, red arrow). The proportion of cells that passed the R-point (BrdU-positive) correlated closely with the proportion of cells with E2F levels in the ON state, in the same concentration-dependant manner with a common bistable range (0.2–1%; Fig. 4b). This correlation was further confirmed at the single-cell level. That is, in a final serum gradient following an initial serum pulse, the very cells that had E2F expression in the activated state (Fig. 4c, *y* axis) were those able to pass the R-point (indicated by their increased DNA content to 3–4*n*, Fig. 4c, *x* axis).

Lastly, we found that the duration of serum stimulation required to turn ON the bistable Rb–E2F switch underlies the traverse through the R-point. A key characteristic of the Rb–E2F bistable switch, as indicated by the model, is that its activation requires a critical duration of strong serum stimulation (T_r; Fig. 5a). After this critical time, E2F steady-state becomes independent of sustained serum-stimulation. This prediction was again confirmed in our experiments. When quiescent cells were treated with 20% serum for various durations, we found that a critical duration of 2–4 h was required to activate E2F expression and to drive R-point traverse in most cells (Fig. 5b). At the single-cell level, the critical duration of stimulation required for E2F activation (Fig. 5c, *y* axis) was found to underlie that required for passing the R-point (Fig. 5c, *x* axis). This result also suggests that traverse of the R-point is established when the Rb–E2F bistable switch is just turned ON (2–4 h for most cells in our cell lines; Fig. 5c), which could occur much earlier, before the E2F accumulation becomes noticeable (>10 hr, Supplementary Information, Fig. S1).

Control of the R-point at the G1–S transition of the mammalian cell cycle is a complex process, likely to involve many other regulatory activities not included in our model. Our work here, together with other studies, nevertheless suggests that the Rb–E2F bistable switch, by its unique properties, is fundamental in establishing the R-point. First, it is 'indispensable': the R-point control was lost completely in cells with knockout of all Rb family members[30,31]. In addition, the ability of a cell to pass the R-point to enter the cell cycle was completely blocked when all E2F activators were knocked out[20]. Second, it is 'sufficient': introducing E2F activity alone can induce quiescent cells to enter S-phase[19]. In addition, cells with E2F turned ON were the very ones that were able to pass the R-point, despite varying strengths and duration of growth stimulation (Figs 4, 5). To our knowledge, the Rb–E2F network is the only system identified in the mammalian cell-cycle machinery that is both indispensable and sufficient for the R-point control.

Our results indicate that the Rb–E2F pathway functions as a bistable switch in response to growth stimulation. The all-or-none and, especially, history-dependent switching behaviour of this gene network (in terms of E2F accumulation in each individual cell) provides a mechanistic explanation for the R-point concept. Our work provides a foundation for future studies that will carefully analyse the contribution of individual components in the Rb–E2F gene network in achieving E2F bistability (for example, the relative contributions of Myc feed-forward regulation and E2F-coupled positive-feedbacks, see Supplementary Information Discussion and Supplementary Information, Fig. S6). Such studies will provide further detailed understanding how precisely the R-point is controlled in mammalian cells. □

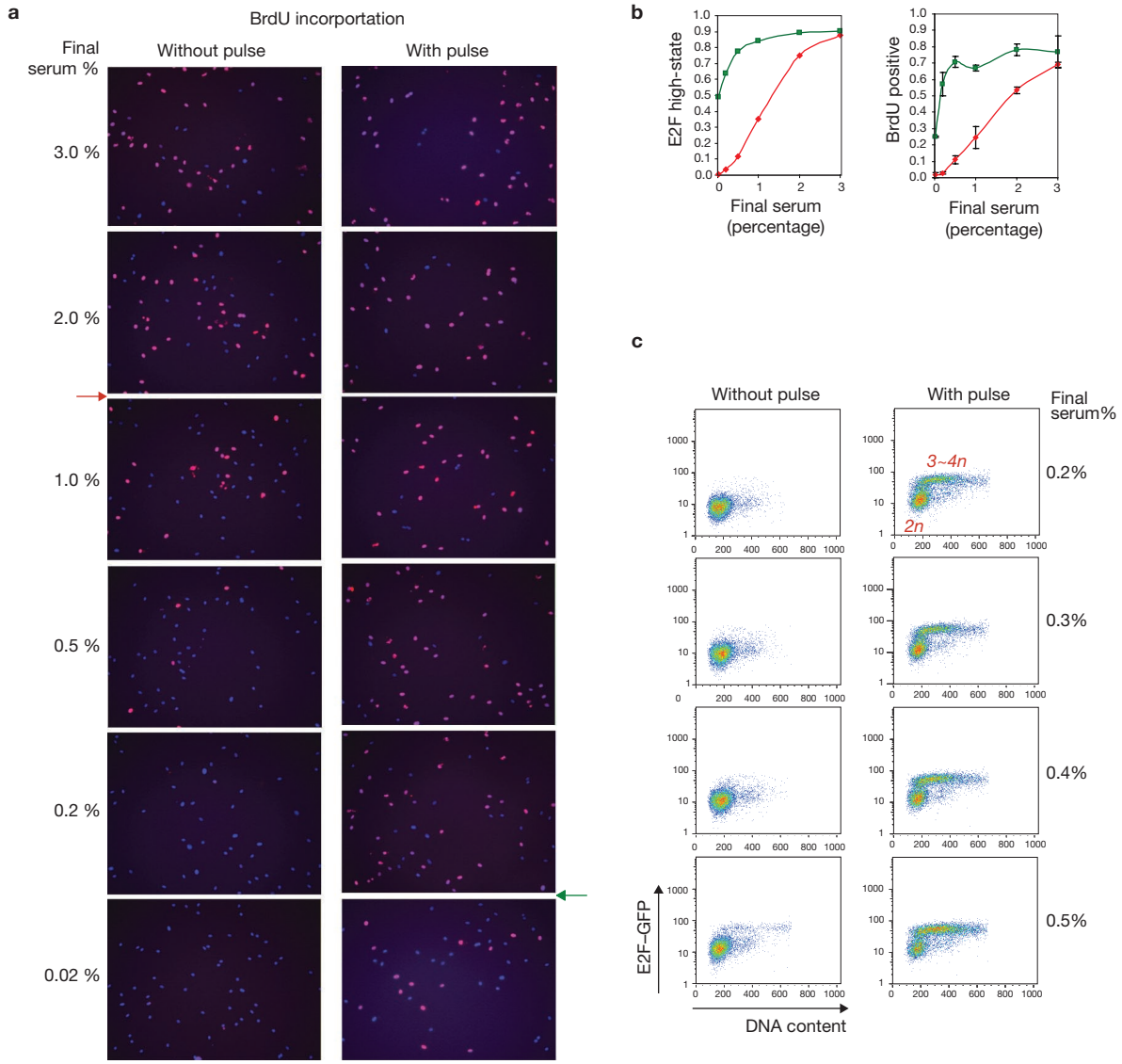

Figure 4 Bistable E2F accumulation underlies R-point traverse in response to graded serum-inputs. (**a**–**c**) Cells were serum-starved and quiescent at time 0. (**a**) BrdU incorporation. Cells (E2F clone no. 23) were treated as described in Fig. 3c (but synchronized at G2–M with nocodazole to allow S-phase BrdU incorporation, and assayed at 30 h). BrdU was included from 5–30 h. Blue dots are DAPI-stained cell nuclei. Magenta dots indicate superimposed BrdU cells. (**b**) Correlation between bistable E2F activation and BrdU incorporation. Proportion of cells with E2F in the ON state (left), calculated from the corresponding E2F distribution in Fig. 3c. Proportion of BrdU-positive cells (right). Data are mean ± s. e. m. of the proportion of BrdU-positive cells, counted from three independent microscopic fields, under treatment conditions described in **a**. (**c**) Single-cell level correlation. Cells were treated with serum at final concentrations as indicated, with or without an initial serum pulse (10% for 6 h). Cells were synchronized at G2–M by nocodazole at the time of assay (27 hr). DNA content was labelled with 7-AAD.

METHODS

GFP reporter system. An expression cassette encoding a destabilized EGFP protein with a half-life of approximately 2 hr (d2GFP; Clontech) was cloned after promoters of E2F and CycD, as described in the Supplementary Information Methods.

Cell culture, synchronization and serum stimulation. Cells were regularly passed in Dulbecco's Modified Eagle's Medium (DMEM) medium (No. 31053, Gibco/Invitrogen) supplemented with 10% of bovine growth serum (BGS, No. SH30541 from Hyclone). Puromycin (2.5 μg ml^{-1}) was added for the d2GFP reporter cell lines. In typical experiments, to measure the endpoint levels of E2F-d2GFP or CycD–d2GFP responses, cells were first synchronized at the quiescent phase. To this end, growing cells were trypsinized, washed once with DMEM medium, resuspended in DMEM supplemented with 0.02% BGS (starvation medium), plated at a density of approximately 10^5 cells per well and cultured for 1–2 days in 6-well cell culture plates (No. 353046, Falcon/BD Biosciences). For serum stimulation, starvation medium was replaced with DMEM medium containing BGS at the indicated concentrations. Hydroxyurea (2 mM) or nocodazole (0.1 μg ml^{-1}) was included in culture medium as indicated, to synchronize cells at the G1–S or G2–M phases, respectively.

Flow cytometry. Cells (cultured in 6-well plate) were collected at the indicated times by trypsinization. For GFP-intensity measurement, cells were fixed directly with 1% formaldehyde in PBS. For GFP and 7-actinoactinomycin D (7-AAD) double detection, cells were first resuspended in 20 μl of BD Cytofix/Cytoperm Buffer (No. 554722, BD Biosciences), left at room temperature for 15 min, combined with 200 μl of staining buffer (3% heat-inactivated FBS plus 0.09% sodium azide in PBS) and centrifuged at 960*g* for 2 min. Cells were subsequently resuspended with 20 μl of freezing buffer (10% DMSO and 90% heat-inactivated FBS), placed at –80°C for 1 h, thawed and immediately combined with staining buffer

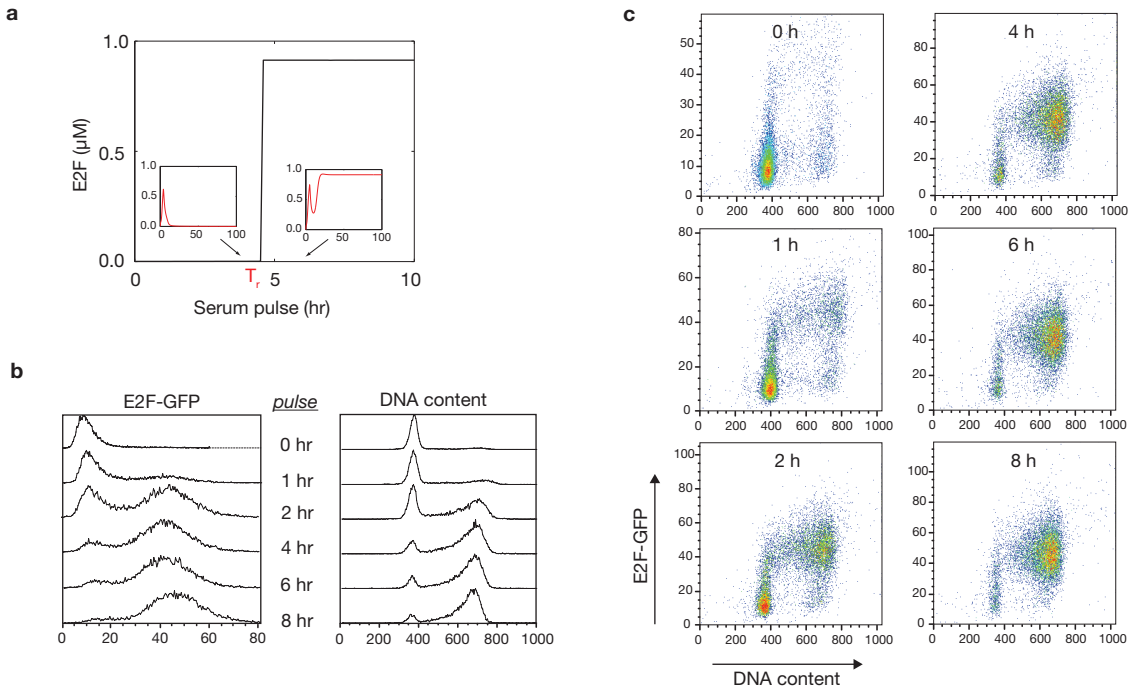

Figure 5 Critical timing in activating the bistable Rb–E2F switch underlies R-point traverse. (**a**–**c**) Cells were serum-starved and quiescent at time 0. (**a**) Model prediction of the critical serum duration (T_r) required for E2F activation (pulse strength, 20%, final serum concentration, 0.3%). When the pulse duration is shorter than T_r, the final E2F level will return to the OFF state (left inset); otherwise, the final E2F level will reach and stay at the same ON state, independent of sustained serum-stimulation (right inset). (**b**, **c**) Quiescent cells were stimulated with a serum pulse (20%) for the durations indicated, followed by incubation in 0.3% serum. Cells were synchronized at G2–M by nocodazole at time of assay (26 h). DNA content was labelled with 7-AAD.

and centrifuged, as above. Finally, cells were resuspended with 4 μl of 7-AAD in 200 μl of staining buffer. For each sample, approximately 10,000 cells were measured using a BD FACScan flow cytometer (BD Biosciences), and analysed using FlowJo software (v7.2, Tree Star).

Microscopy and immunostaining. For BrdU incorporation, cells were serum-starved and stimulated as described above. BrdU (50 μM, No. 280879, Roche Applied Science) was included in the culture medium at the indicated times. Cells were fixed and permeabilized as described previously (Supplementary Information, ref. 5). Incorporated BrdU was detected using an anti-BrdU antibody (1:5, No. RPN202, Amersham Biosciences), followed by secondary antibody (Texas Red-conjugated anti-mouse, 1:500, No. TI-2000, Vector Laboratories), according to the manufacturer's instructions. Cell nuclei were stained with DAPI (0.1 μg ml^{-1}, No. 236276, Roche Applied Science) and assayed using a Leica DMI 6000 B inverted fluorescent microscope. Images were taken using a Leica HC PLAN APO ×10/0.40 objective lens, with Semrock BrightLine filters for DAPI and Texas Red detections. All images were captured using a Hamamatsu ORCA-AG digital camera with Compix SimplePCI imaging software (v6.0), with binning at 4, offset at 255, gain at 0, exposure at 0.04 s for DAPI and 0.6 s for Texas Red. Images were further adjusted for contrast in SimplePCI using × Squared method (with low to high range of 0–180). Three independent fields were counted for the percentage of BrdU positive cells under each treatment.

For GFP detection, cells were serum starved in 0.02% BGS plus fibronectin (1 μg ml^{-1}, No. F1141, Sigma) for 1.5 days in glass-bottom microwell dishes (No. P6G-1.5-20-F, MatTek), then further cultured in original starvation medium or 20% BGS for 19–22 hours. Cells were washed once with, and finally placed into PBS to minimize autofluorescence in growth medium, and assayed immediately using a Leica microscope as above. Images were taken using a Leica N PLAN L ×20/0.40 objective lens with phase-contrast or a Semrock BrightLine GFP filter. All images were captured using a Hamamatsu camera as above, with binning at 4, offset at 255, gain at 0, exposure at 0.01 s for phase images and 0.2–1.0 s for GFP images. Images were further adjusted for contrast in SimplePCI using a Normal Linear method.

Real time RT-PCR assay. Total RNA was collected using RNeasy Mini Kit (Qiagen) according to the manufacturer's instructions. Quantitative, real time RT-PCR was performed with the ABI PRISM 7900HT Sequence Detection System (Applied Biosystems) with QuantiTect SYBR Green RT-PCR Kit (Qiagen) according to the manufacterer's protocol. The same amount (50 ng) of RNA template was used for each assay. In addition, real time RT-PCR level of β-actin was used as an internal loading control. Primer sets for RT-PCR include 5'TTGACCCCTCTGGATTTCTG3' and 5'CCCTTTGGTCTGCTCAATGT3' (for E2F1), 5'GCGTACCCTGACACCAATCT3' and 5'CTCTTCGCACTTCTGCTCCT3' (for CycD1), 5'GATCTGGCACCACACCTTCT3' and 5'GGGGTGTTGAAGGTCTCAAA3' (mouse β-actin primers, verified for amplification efficiency and specificity in REF52 cells).

Model development. We developed a simplified mathematical model to account for the key interactions outlined in Figure 1B. For details see Supplementary Information Methods.

Note: Supplementary Information is available on the Nature Cell Biology website.

ACKNOWLEDGEMENTS

We thank W. Zhu, L. Kong, R. Rempel, T. Hallstrom, and C. Tan for comments on the manuscript. We also thank Y. Leung, S. Angus, E. Andrechek, Q. Wang, L. Jakoi, K. Culler and H. Zhang for their help. This project was supported by grants from the NIH 5-U24-CA112952-03 (to J.R.N.), NSF BES-0625213 (to L.Y.) and a David and Lucile Packard Fellowship (to L.Y.).

AUTHOR CONTRIBUTIONS

G. Y., L. Y. and J. R. N. conceived the project; T. L., L. Y. and G. Y. performed the mathematical modelling; G. Y. performed the experiments. G. Y., L. Y. and J. R. N. analysed the data. S. M. contributed materials and reagents. G. Y., T. L., L. Y. and J. R. N wrote the paper.

Published online at http://www.nature.com/naturecellbiology/
Reprints and permissions information is available online at http://npg.nature.com/reprintsandpermissions/

1. Malumbres, M. & Barbacid, M. To cycle or not to cycle: a critical decision in cancer. *Nature Rev. Cancer* **1,** 222–231 (2001).
2. Weinberg, R. A. *The biology of cancer*. (Garland Science, New York, 2007).
3. Sears, R. C. & Nevins, J. R. Signaling networks that link cell proliferation and cell fate. *J. Biol. Chem.* **277,** 11617–11620 (2002).
4. Frolov, M. V. & Dyson, N. J. Molecular mechanisms of E2F-dependent activation and pRB-mediated repression. *J. Cell Sci.* **117,** 2173–2181 (2004).
5. Attwooll, C., Lazzerini Denchi, E. & Helin, K. The E2F family: specific functions and overlapping interests. *EMBO J.* **23,** 4709–4716 (2004).
6. Sherr, C. J. & Roberts, J. M. CDK inhibitors: positive and negative regulators of G1-phase progression. *Genes Dev.* **13,** 1501–1512 (1999).
7. Zetterberg, A., Larsson, O. & Wiman, K. G. What is the restriction point? *Curr. Opin. Cell Biol.* **7,** 835–842 (1995).
8. Pardee, A. B. A restriction point for control of normal animal cell proliferation. *Proc. Natl Acad. Sci. USA* **71,** 1286–1290 (1974).
9. Zetterberg, A. & Larsson, O. Kinetic analysis of regulatory events in G1 leading to proliferation or quiescence of Swiss 3T3 cells. *Proc. Natl Acad. Sci. USA* **82,** 5365–5369 (1985).
10. Xiong, W. & Ferrell, J. E., Jr. A positive-feedback-based bistable 'memory module' that governs a cell fate decision. *Nature* **426,** 460–465 (2003).
11. Sha, W. *et al.* Hysteresis drives cell-cycle transitions in *Xenopus laevis* egg extracts. *Proc. Natl Acad. Sci. USA* **100,** 975–980 (2003).
12. Ozbudak, E. M., Thattai, M., Lim, H. N., Shraiman, B. I. & Van Oudenaarden, A. Multistability in the lactose utilization network of *Escherichia coli*. *Nature* **427,** 737–740 (2004).
13. Paliwal, S. *et al.* MAPK-mediated bimodal gene expression and adaptive gradient sensing in yeast. *Nature* **446,** 46–51 (2007).
14. Aguda, B. D. & Tang, Y. The kinetic origins of the restriction point in the mammalian cell cycle. *Cell Prolif.* **32,** 321–335 (1999).
15. Novak, B. & Tyson, J. J. A model for restriction point control of the mammalian cell cycle. *J. Theoret. Biol.* **230,** 563–579 (2004).
16. Hatzimanikatis, V., Lee, K. H. & Bailey, J. E. A mathematical description of regulation of the G1–S transition of the mammalian cell cycle. *Biotech. Bioeng.* **65,** 631–637 (1999).
17. Qu, Z., MacLellan, W. R. & Weiss, J. N. Dynamics of the cell cycle: checkpoints, sizers, and timers. *Biophys. J.* **85,** 3600–3611 (2003).
18. Thron, C. D. Bistable biochemical switching and the control of the events of the cell cycle. *Oncogene* **15,** 317–325 (1997).
19. Johnson, D. G., Schwarz, J. K., Cress, W. D. & Nevins, J. R. Expression of transcription factor E2F1 induces quiescent cells to enter S phase. *Nature* **365,** 349–352 (1993).
20. Wu, L. *et al.* The E2F1-3 transcription factors are essential for cellular proliferation. *Nature* **414,** 457–462 (2001).
21. Leung, J. Y., Ehmann, G. L., Giangrande, P. H. & Nevis, J. R. A role for Myc in facilitating transcription activation by E2F. *Oncogene*, advance online publication, doi:10.1038/onc.2008.55 (2008).
22. Tyson, J. J., Chen, K. C. & Novak, B. Sniffers, buzzers, toggles and blinkers: dynamics of regulatory and signaling pathways in the cell. *Curr. Opin. Cell Biol.* **15,** 221–231 (2003).
23. Ferrell, Jr, J. E.. Self-perpetuating states in signal transduction: positive feedback, double-negative feedback and bistability. *Curr. Opin. Cell Biol.* **14,** 140–148 (2002).
24. Gardner, T. S., Cantor, C. R. & Collins, J. J. Construction of a genetic toggle switch in Escherichia coli. *Nature* **403,** 339–342 (2000).
25. Isaacs, F. J., Hasty, J., Cantor, C. R. & Collins, J. J. Prediction and measurement of an autoregulatory genetic module. *Proc. Natl Acad. Sci. USA* **100,** 7714–7719 (2003).
26. Rao, C. V., Wolf, D. M. & Arkin, A. P. Control, exploitation and tolerance of intracellular noise. *Nature* **420,** 231–237 (2002).
27. Longo, D. & Hasty, J. Dynamics of single-cell gene expression. *Mol. Syst. Biol.* **2,** 64 (2006).
28. Bean, J. M., Siggia, E. D. & Cross, F. R. Coherence and timing of cell cycle start examined at single-cell resolution. *Mol. Cell* **21,** 3–14 (2006).
29. Matsushime, H., Roussel, M. F., Ashmun, R. A. & Sherr, C. J. Colony-stimulating factor 1 regulates novel cyclins during the G1 phase of the cell cycle. *Cell* **65,** 701–713 (1991).
30. Dannenberg, J. H., van Rossum, A., Schuijff, L. & te Riele, H. Ablation of the retinoblastoma gene family deregulates G(1) control causing immortalization and increased cell turnover under growth-restricting conditions. *Genes Dev.* **14,** 3051–3064 (2000).
31. Sage, J. *et al.* Targeted disruption of the three Rb-related genes leads to loss of G(1) control and immortalization. *Genes Dev.* **14,** 3037–3050 (2000).

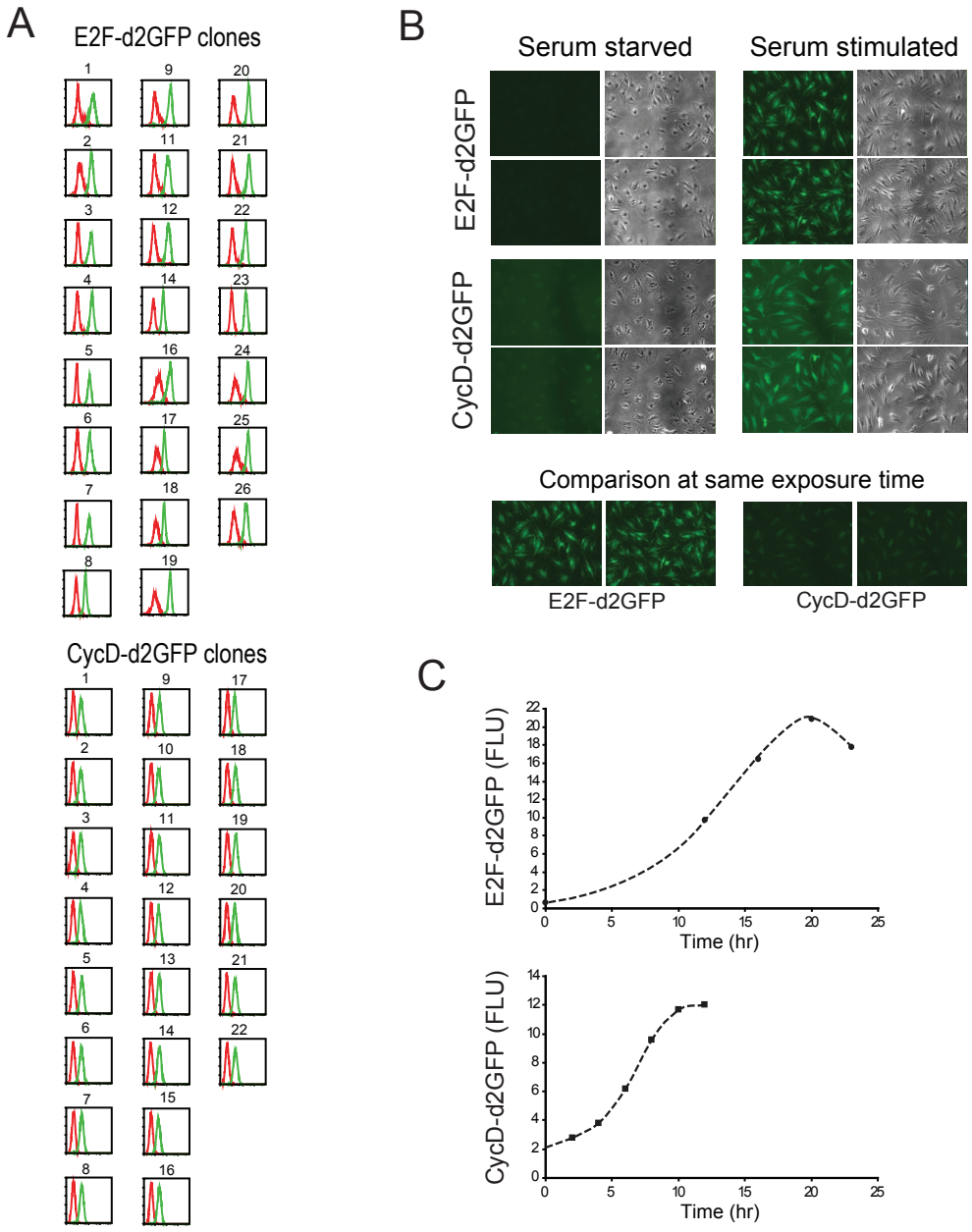

Figure S1 Establishment of single reporter cell clones. **A.** Flow cytometry of individual clone. Red curve, serum starved cells. Green curve, serum stimulated cells. Each curve represents d2GFP distribution from ~10,000 cells. Missing clone numbers indicate those excluded initially by phase microscopy for nonhomogeneous morphology. **B.** Fluorescent microscopy of serum response of E2F-d2GFP and CycD-d2GFP cells. (Upper) One representative clone (E2F: #23, CycD: #5) of each reporter cell line was shown. For each clone, two independent fields were imaged at both serum starvation (0.02% BGS) and serum stimulation (20% BGS) conditions, with GFP image (left) and phase contrast (right). Fluorescent microscopy exposure time: E2F-d2GFP, 0.2 second; CycD-d2GFP, 1.0 second. (Lower) Direct comparison of E2F-d2GFP and CycD-d2GFP cell serum responses, with same fields as above (serum stimulated) imaged with exposure time = 0.2 second. See Methods for additional imaging details. **C.** Temporal responses of d2GFP reporter cell lines. Serum starved cells were stimulated with 10% BGS, harvested at indicated time points, and subjected to flow cytometry. GFP intensities were normalized by subtracting background autofluorescence (as measured in parental REF52 cells at each corresponding condition). Considering the time delay for GFP reporter protein translation and maturation, the half-maximum activation times (E2F-d2GFP, ~13 hr; CycD-d2GFP, ~6 hr) were consistent with the well-studied endogenous gene expression of E2F1 and CycD1.[1,22,23]

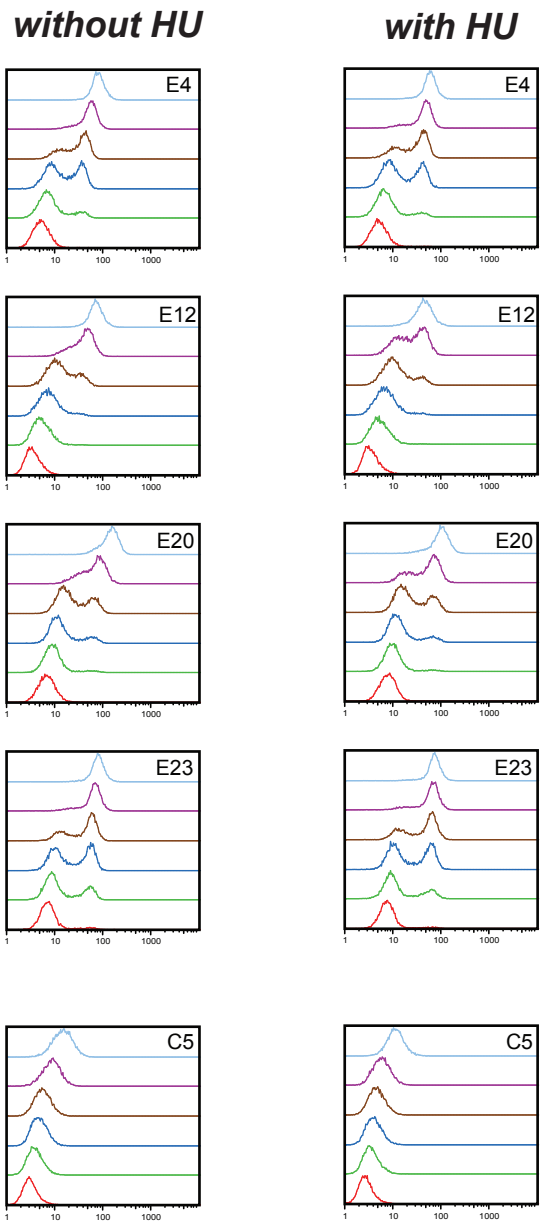

Figure S2 Serum dose response measurement with or without HU. Cells were serum starved at 0.02% BGS for 1 day and subsequently stimulated with BGS at indicated concentrations. To one half of the cells, Hydroxyurea (HU) was included in the culture medium throughout the serum stimulation process to synchronize cells at G1-S at time of assay (24 hr). To the other half of cells, HU was not applied. Each histogram represents the d2GFP distribution from ~10,000 cells.

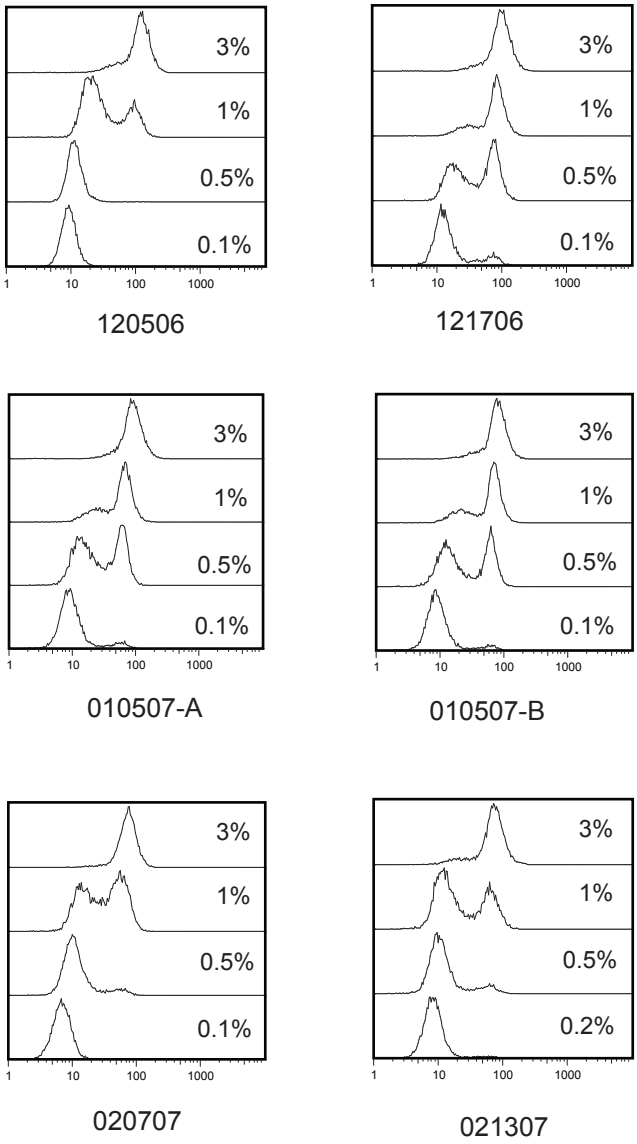

Figure S3 Repeated measurements of E2F-d2GFP dose response. Cells from one single cell clone (#23) were tested at different days as indicated. At each test, cells were first synchronized to quiescence by serum starvation (0.02% BGS, 1~1.5 days), then stimulated with BGS at indicated concentrations for 24~25 hours. GFP intensity was measured by flow cytometry. Each histogram represents the d2GFP distribution from ~10,000 cells.

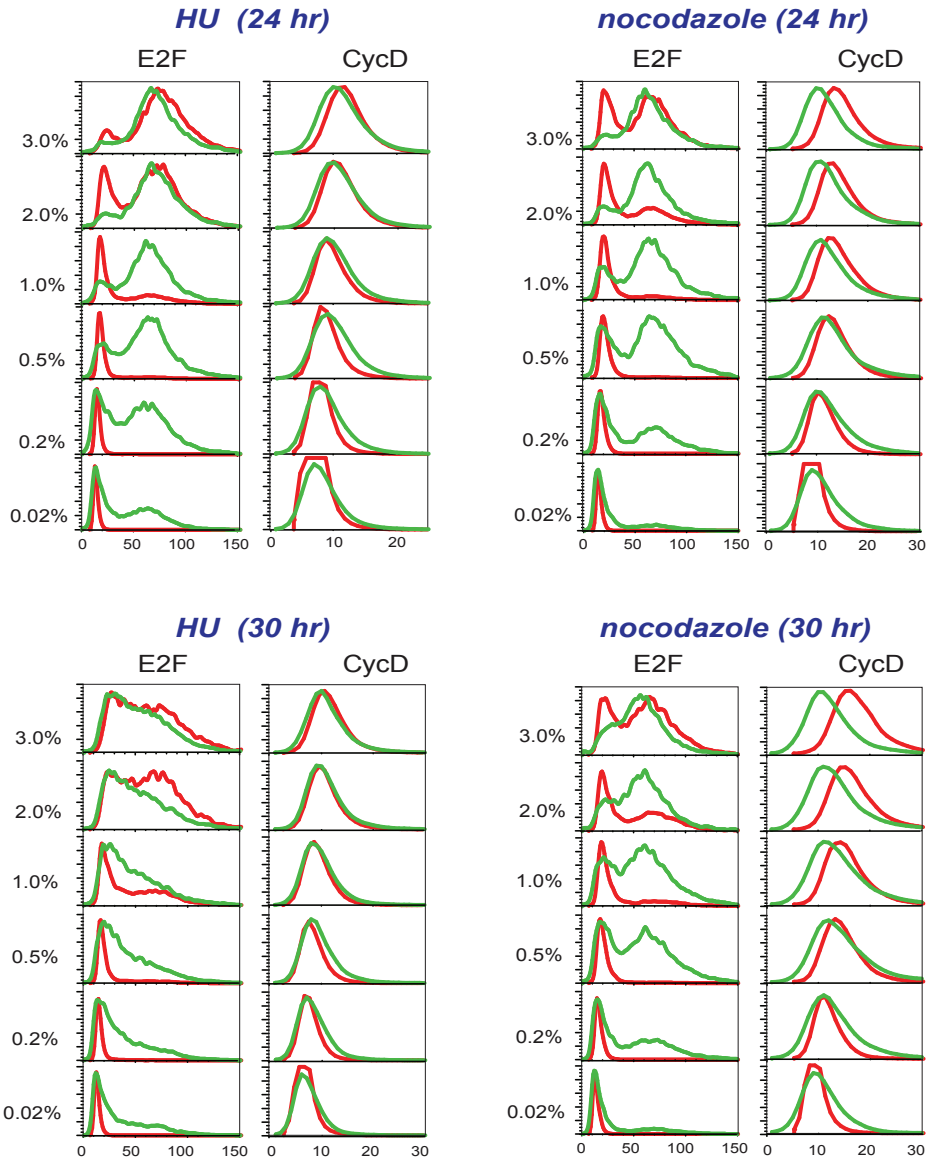

Figure S4 E2F history dependence. Quiescent E2F-d2GFP and CycD-d2GFP Cells were stimulated with BGS at indicated concentrations, with (green curves) or without (red curves) an initial strong serum pulse (20% for 5 hours). HU or nocodazole (as indicated) was applied to synchronize cells at the G1-S or G2-M phase. Each histogram represents the distribution of GFP signals from ~10,000 cells (E2F clone #23, CycD clone #5) after baseline correction (Figure S5), measured at 24 or 30 hours (as indicated) after serum stimulation. Regardless of synchronization method and time of measurement, at serum concentrations between 0.2% and 1.0%, the E2F-d2GFP signal in considerably larger amount of cells were at ON-state with the initial pulse stimulation (green), as compared to that without the pulse stimulation (red). In contrast, the CycD-d2GFP signal in cells with pulse stimulation (green) was at the same average level as that in cells without pulse stimulation (red), or reduced to even lower level probably due to drug toxicity and downstream gene regulation.

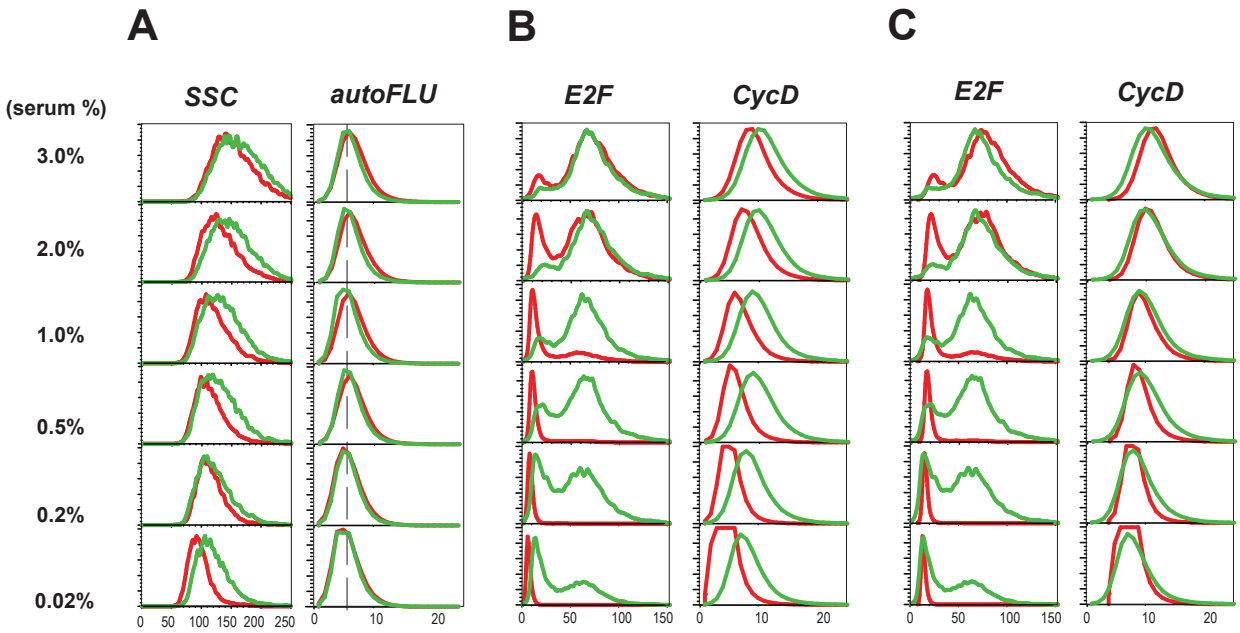

Figure S5 Baseline correction for pulse stimulation. In serum pulse stimulation protocol (as in Figure 3A), treatment with (green curves) or without (red curves) the initial serum pulse could lead to the difference in cellular physiological state, as reflected in the systematic discrepancy in cell side-scattering (SSC) **(A)**. This physiological difference likely contributed to the baseline shift in both the E2F-d2GFP and CycD-d2GFP levels, between cells with and without initial pulse stimulation **(B)**. Other contributing factors might include the delay in GFP protein degradation, and residual growth factors not completely washed off, following the serum pulse. The autofluorescence background was unlikely a contributing factor because its levels were basically unchanged at all tested conditions, as measured with the parental REF52 cells **(A)**. To correct for the systematic baseline shift, distribution curves with or without initial pulse stimulation (for both E2F-d2GFP and CycD-d2GFP) were aligned by their modes at the starvation condition (0.02% BGS), as shown in **(C)**.

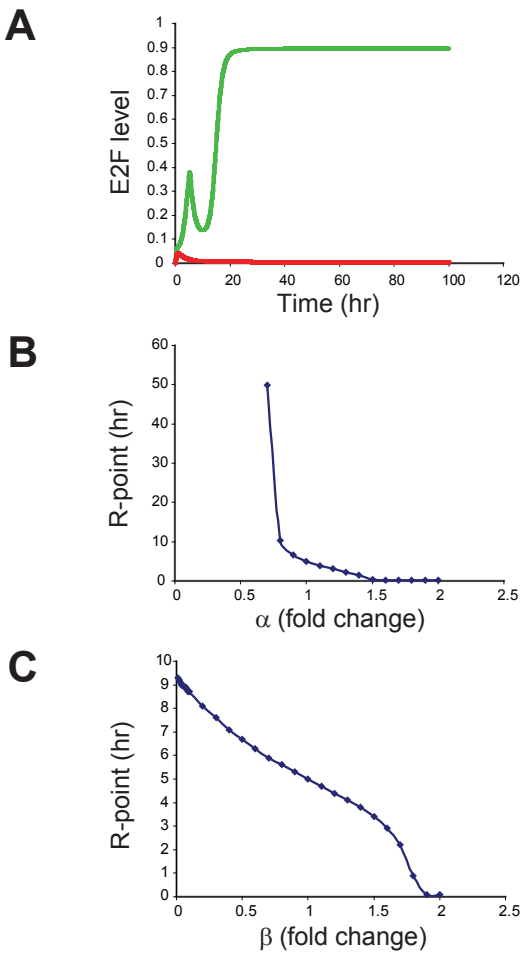

Figure S6 Modulation of the R-point via positive feedback and feed-forward modules. **A.** The E2F positive feedback alone (without direct Myc modulation), if sufficiently strong, can generate a history-dependent bistable behavior. E2F can be at either high or low state depending on the input pattern. An initial serum pulse (10% for 6 hr) activates the system from the low state to the high state (green). Absence of the initial pulse maintains E2F at its low level (red). **B.** Modulation of the R-point via the E2F positive feedback module, evaluated by changing the feedback strength (α). **C.** Modulation of the R-point via the Myc feedforward module, evaluated by changing the feedforward strength (β). **A ~ C.** kEF (=0.28 μM/hr) and kb (=0.02 μM/hr) values were adjusted to maintain the default R-point value at 5 hours as in the base case.

Table S1. The mathematical model for the Rb-E2F pathway.

$\frac{d[M]}{dt} = \frac{k_M[S]}{K_S+[S]} - d_M[M]$
$\frac{d[CD]}{dt} = k_E\left(\frac{M}{K_M+[M]}\right)\left(\frac{[E]}{K_E+[E]}\right) + \frac{k_b[M]}{K_M+[M]} + \frac{k_{p1}[CD][RE]}{K_{CD}+[RE]} + \frac{k_{P2}[CE][RE]}{K_{CE}+[RE]}$ $-d_E[E] - k_{RE}[R][E]$
$\frac{d[CD]}{dt} = \frac{k_{CD}[M]}{K_M+[M]} + \frac{k_{CDS}[S]}{K_S+[S]} - d_{CD}[CD]$
$\frac{d[CE]}{dt} = \frac{k_{CE}[E]}{K_E+[E]} - d_{CE}[CE]$
$\frac{d[R]}{dt} = k_R + \frac{k_{DP}[RP]}{K_{RP}+[RP]} - k_{RE}[R][E] - \frac{k_{P1}[CD][R]}{K_{CD}+[R]} - \frac{k_{P2}[CE][R]}{K_{CE}+[R]} - d_R[R]$
$\frac{d[RP]}{dt} = \frac{k_{P1}[CD][R]}{K_{CD}+[R]} + \frac{k_{P2}[CE][R]}{K_{CE}+[R]} + \frac{k_{P1}[CD][RE]}{K_{CD}+[RE]} + \frac{k_{P2}[CE][RE]}{K_{CE}+[RE]} - \frac{k_{DP}[RP]}{K_{RP}+[RP]} - d_{RP}[RP]$
$\frac{d[RE]}{dt} = k_{RE}[R][E] - \frac{k_{P1}[CD][RE]}{K_{CD}+[RE]} - \frac{k_{P2}[CE][RE]}{K_{CE}+[RE]} - d_{RE}[RE]$

Variables are:

S: growth signals (e.g. serum)

M: Myc

E: E2F

CD: CycD

CE: CycE

R: Rb

RP: Phosphorylated Rb

RE: Rb-E2F complex

Initial condition:

[Rb] = 0.55 μM; [Rbp] = [E2F] = [Myc] = [CycD] = [CycE] = 0 μM

Underlying reactions for these ODEs are defined in Table S2.

Parameters are defined in Table S3.

Table S2. Reaction kinetics for the model

Reaction	Kinetics	Description and notes
$* \xrightarrow{S} M$	$\frac{k_M[S]}{K_S+[S]}$	Myc synthesis driven by growth signals (S)
$* \xrightarrow{S} CD$	$\frac{k_{CDS}[S]}{K_S+[S]}$	CycD synthesis driven by growth signals
$* \xrightarrow{M,E} E$	$k_E\left(\frac{[M]}{K_M+[M]}\right)\left(\frac{[E]}{K_E+[E]}\right)+\frac{k_b[M]}{K_M+[M]}$	E2F synthesis by a synergy between Myc and E2F autocatalysis. Since neither Myc nor E2F forms a homodimer, we assumed no cooperativity in gene activation mediated by these factors, and used the Hill coefficient of 1.0. Using Hill coefficient greater than 1.0 will not change the qualitative behavior of system dynamics
$* \xrightarrow{E} CE$	$\frac{k_{CE}[E]}{K_E+[E]}$	CycE synthesis driven by E2F
$* \xrightarrow{M} CD$	$\frac{k_{CD}[M]}{K_M+[M]}$	CycD synthesis driven by Myc
$* \longrightarrow R$	k_R	Constitutive Rb synthesis
$RE \xrightarrow{CD,CE} E+RP$	$\frac{k_{P1}[CD][RE]}{K_{CD}+[RE]}+\frac{k_{P2}[CE][RE]}{K_{CE}+[RE]}$	E2F dissociation from Rb-E2F complex by CycD- and CycE-mediated phosphorylation
$E+R \longrightarrow RE$	$k_{RE}[R][E]$	E2F titration by Rb via E2F-Rb complex formation
$R \xrightarrow{CD,CE} RP$	$\frac{k_{P1}[CD][R]}{K_{CD}+[R]}+\frac{k_{P2}[CE][R]}{K_{CE}+[R]}$	Rb phosphorylation by CycD and CycE
$RP \longrightarrow R$	$\frac{k_{DP}[RP]}{K_{RP}+[RP]}$	Rb dephosphorylation
$M \longrightarrow *$	$d_M[M]$	Myc decay
$E \longrightarrow *$	$d_E[E]$	E2F decay
$CE \longrightarrow *$	$d_{CE}[CE]$	CycE decay
$CD \longrightarrow *$	$d_{CD}[CD]$	CycD decay
$R \longrightarrow *$	$d_R[R]$	Rb decay
$RP \longrightarrow *$	$d_{RP}[RP]$	Phosphorylated Rb decay
$RE \longrightarrow *$	$d_{RE}[RE]$	Rb-E2F complex decay

Table S3. Parameters for the model

Rate constants		Parameter values, sources, and notes
k_E	0.4 μM/hr	These values were adjusted together so that: (1) The maximum E2F level is higher than the maximum CycD level (based on our experimental observations) (2) E2F activation threshold is about 1% serum (3) The simulated E2F level will be around the corresponding Michaelis-Menten parameter (K_E)
k_M	1.0 μM/hr	
k_{CD}	0.03 μM/hr	
k_{CDS}	0.45 μM/hr	
k_R	0.18 μM/hr	
k_{RE}	180 μM/hr	
k_b	0.003 μM/hr	
K_S	0.5 μM	
k_{CE}	0.35 μM/hr	Assumed to be similar to k_{EF}
d_M	0.7/hr	Myc half-life = 60 min [9-11]
d_E	0.25/hr	E2F half-life = 2~3 hr [12]
d_{CD}	1.5/hr	CycD half-life = 25~30 min [13, 14]
d_{CE}	1.5/hr	CycE half-life = 30 min [15, 16]
d_R	0.06/hr	Rb half-life = 12 hours [17]
d_{RP}	0.06/hr	Assumed to be the same as d_R
d_{RE}	0.03/hr	Rb-E2F half-life = 6 hours: The Rb-E2F complex assumed to be more stable than Rb alone [18]
k_{P1}^*, k_{P2}^*	18/hr	Typical value phosphorylation rate constant [19] is 3600/hr
k_{DP}^*	3.6 μM/hr	Typical value for dephosphorylation rate assuming a constant phosphatase concentration [19] is 720 μM/hr
K_M	0.15 μM	Estimated based on measured Myc/Max –DNA dissociation constant [20]
K_E	0.15 μM	Assumed to be the same as K_M
K_{CD}	0.92 μM	Experimentally measured [21, 22]
K_{CE}	0.92 μM	Assumed to be the same as CycD
K_{RP}	0.01 μM	Typical value for Michaelis-Menten parameter for dephosphorylation [19]

* Typical values of phosphorylation and dephosphorylation rate constants results in a stiff model, which drastically slows down the calculation. We have found that the overall dynamics is insensitive to the overall rates of the phosphorylation and dephosphorylation reactions, as long as they are balanced. Thus we have reduced the corresponding rate constants by 200 fold to speed up calculation. Proportionally increasing these parameters has no significant impact on the overall system dynamics.

Materials and Methods

GFP reporter system. An expression cassette encoding a destabilized EGFP protein with ~ 2 hr half-life (d2GFP; Clontech, Mountain View, CA) was cloned downstream of the human E2F1 promoter[1], and into a pQCXIP retroviral vector (Clontech, Mountain View, CA). This recombined retroviral construct was transfected into an ecotropic packaging cell line, Plat-E[2]. After 36 hours, the culture medium containing retrovirus particles was applied to infect REF-52 cells[3]. Stable E2F-d2GFP integrations were selected by puromycin resistance (2.5 μg/ml). In this E2F-d2GFP reporter system, the destabilized d2GFP, rather than standard GFP, was employed to better monitor the kinetics of E2F1 transcription (representing all E2F activators in this study). Furthermore, the pQCXIP retroviral vector features self-inactivated 5' LTR promoter activity to minimize its transcriptional interference. In parallel, a CycD-d2GFP control system was constructed, differing only in the promoter sequence (CycD1[4] instead of E2F1). Next, single cell clones were established from both cell lines by fluorescence-activated cell sorting (FACS) of single cell into 96-well plates, and subsequently expanded. These cell clones were further assayed with phase-contrast microscopy and flow cytometry; those that exhibited high degree of homogeneity (both at cell morphology and GFP signal distribution) were chosen for subsequent experiments.

Cell culture, synchronization, and serum stimulation. Cells were regularly passed in Dulbecco's Modified Eagle's Medium (DMEM) medium (#31053, Gibco/Invitrogen, Carlsbad, CA) supplemented with 10% of bovine growth serum (BGS, #SH30541 from Hyclone, Logan, UT). Puromycin (2.5 μg/ml) was applied in addition for d2GFP reporter cell lines. In typical experiments to measure the endpoint

levels of E2F-d2GFP or CycD-d2GFP dose response, cells were first synchronized at the quiescent phase. To this end, growing cells were trypsinized, washed once with DMEM medium, and then resuspended in DMEM supplemented with 0.02% BGS (starvation medium), plated at a density of ~ 10^5 cells/well and cultured for 1~2 days in 6-well cell culture plates (#353046, Falcon/BD Biosciences, San Jose, CA). For serum stimulation, starvation medium was replaced with DMEM medium containing BGS at indicated concentrations. Hydroxyurea (HU; 2 mM) or nocodazole (0.1 μg/ml) was included in culture medium as indicated to synchronize cells at the G1-S or G2-M phases, respectively.

Flow cytometry. Cells (cultured in 6-well plate) were harvested at indicated times by trypsinization. For GFP intensity measurement, cells were fixed directly with 1% formaldehyde in PBS. For GFP and 7-AAD double detection, cells were first resuspended in 20 μl of BD Cytofix/Cytoperm Buffer (#554722, BD Biosciences, San Jose, CA), left at room temperature for 15 min, then combined with 200 μl of staining buffer (3% heat inactivated FBS plus 0.09% sodium azide in PBS) and spinned down. Cells were subsequently resuspended with 20 μl of freezing buffer (10% DMSO plus 90% heat inactivated FBS), put at -80 °C for 1 hour, thawed, and promptly combined with staining buffer and spinned down as above. Finally, cells were resuspended with 4 μl of 7-AAD in 200 μl of staining buffer. For each sample, typically ~10,000 cells were measured using a BD FACScan flow cytometer (BD Biosciences), and analyzed using FlowJo software (v7.2, Tree Star, Inc., Ashland, OR).

Microscopy and immunostaining. For BrdU incorporation, cells were serum starved and stimulated as described above. BrdU at 50 μM (#280879, Roche Applied Science, Indianapolis, IN) was included in the culture medium at the indicated time frame.

Cells were fixed and permeabilized as previously described[5]. Incorporated BrdU was detected using anti-BrdU antibody (#RPN202, Amersham Biosciences, Piscataway, NJ), followed by secondary antibody (Texas Red-conjugated anti-mouse; #TI-2000, Vector Laboratories, Burlingame, CA), according to the manufacturers' instructions. DAPI (#236276, Roche Applied Science) at 0.1 μg/ml was applied to stain the cell nucleus. Cells were assayed using a Leica DMI 6000 B inverted fluorescent microscope. Images were taken using a Leica HC PLAN APO 10x/0.40 objective lens, with Semrock BrightLine filters for DAPI and Texas Red detections. All images were captured using a Hamamatsu ORCA-AG digital camera with Compix SimplePCI imaging software (v6.0), with binning = 4, offset = 255, gain = 0, exposure = 0.04 second for DAPI and 0.6 second for Texas Red. Images were further adjusted for contrast in SimplePCI using x Squared method (with low ~ high range of 0 ~ 180). Three independent fields were counted for the percentage of BrdU positive cells under each treatment.

For GFP detection, cells were serum starved in 0.02% BGS plus 1 μg/ml fibronectin (#F1141, Sigma, St. Louis, MO) for 1.5 days in glass-bottom microwell dishes (#P6G-1.5-20-F, MatTek Corp., Ashland, MA), then further cultured in original starvation medium or 20% BGS for 19~22 hours. Cells were washed once with, and finally placed into PBS to minimize autofluorescence in growth medium, and assayed immediately using a Leica microscope as above. Images were taken using a Leica N PLAN L 20x/0.40 objective lens, with phase contrast or a Semrock BrightLine GFP filter. All images were captured using a Hamamatsu camera as above, with binning = 4, offset = 255, gain = 0, exposure = 0.01 second for phase images and 0.2 ~ 1.0 second for GFP images. Phase images and selected GFP images (as

indicated) were further adjusted for contrast in SimplePCI using a Normal Linear method.

Real time RT-PCR assay. Total RNA was collected using RNeasy Mini Kit (Qiagen, Valencia, CA) according to the manufacturer's instructions. Quantitative, real time RT-PCR was performed with the ABI PRISM 7900HT Sequence Detection System (Applied Biosystems, Foster City, CA) with QuantiTect SYBR Green RT-PCR Kit (Qiagen) following the manufacterer's protocol. Same amount (50 ng) of RNA template was used for each assay. In addition, real time RT-PCR level of β-actin was employed as an internal loading control. Primer sets for RT-PCR include 5'TTGACCCCTCTGGATTTCTG3' and 5'CCCTTTGGTCTGCTCAATGT3' (for E2F1), 5'GCGTACCCTGACACCAATCT3' and 5'CTCTTCGCACTTCTGCTCCT3' (for CycD1), 5'GATCTGGCACCACACCTTCT3' and 5'GGGGTGTTGAAGGTCTCAAA3' (mouse β-actin primers, verified for amplification efficiency and specificity in REF52 cells).

Model development. We developed a simplified mathematical model to account for the key interactions outlined in Figure 1B. Our model consists of a set of ordinary differential equations (ODEs) as listed in Table S1. These ODEs were based on kinetics and parameters as shown in Tables S2 and S3. Great care has been taken to estimate basic modeling parameters. Some parameters (e.g., Michaelis-Menten constants and decay rate constants) were obtained from the literature. Some parameters (e.g, maximum phosphorylation and dephosphorylation rate constants) were estimated based on typical values for related or similar kinetic processes. The remaining free parameters (synthesis rates of various components) were constrained with our own measurements. For parameter adjustments and time-course simulations,

we used Dynetica, a graphics-based, integrated simulation platform[6]. We then implemented our model in 'XPP-AUTO' to perform bifurcation analysis[7, 8].

In developing our model, we focused on the role of the Rb-E2F circuit in governing cell cycle entry. As such, our model accounted for cellular dynamics prior to the G1-S transition and neglected downstream gene regulations. Furthermore, we used E2F to generalize all E2F activators (E2F1, E2F2, and E2F3a), and used Rb to represent all pocket proteins (Rb, p107, and p130). In addition, the inhibitory activities of CKIs were lumped into the phosphorylation rate constants of Cyclin-cdk complexes. These simplifications reduced the intricate regulatory network of cell cycle entry to an experimentally tractable model.

Supplementary Discussion

Dissecting contributions of Myc feedforward and E2F positive feedback to R-point control. The contribution of Myc towards E2F activation can potentially be represented in several ways. In Case I, the synergy between E2F and Myc is accounted for by E2F positive feedback coupled with a feed-forward motif (initiating from Myc) as an "AND" gate in terms of its output (E2F). Also Myc contributes to E2F activation through a basal term. This corresponds to the base case used in our mathematical model (Table S2).

$$\text{1) E2F synthesis rate} = k_E\left(\frac{M}{K_M+[M]}\right)\left(\frac{[E]}{K_E+[E]}\right)+\frac{k_b[M]}{K_M+[M]}$$

In Case 2, we assume the E2F positive feedback is not directly affected by Myc but has a maximum strength equivalent to the base case. Consistent with intuition, the positive feedback alone can result in history-dependent switching behavior as shown in Supplementary Figure 6A.

$$\text{2) E2F synthesis rate} = k_E\left(\frac{[E]}{K_E+[E]}\right)+k_b$$

The positive feedback module and the feed-forward module in Case 1 are intricately intertwined, rendering perturbations and interpretation of individual modules extremely challenging. To gain initial insight into Myc's contribution to E2F activation, we decouple the Myc input from the E2F positive feedback (Case 3). We assume that E2F synergy can be accounted for by using an "OR", where the total synthesis rate is a weighted sum of the E2F positive feedback and the Myc input.

$$\text{3) E2F synthesis rate} = k_E\alpha\left(\frac{[E]}{K_E+[E]}\right)+k_b\beta\left(\frac{[M]}{K_M+[M]}\right)$$

This formulation provides a simple way to dissect *in silico* how the Myc input and positive feedback may individually contribute to modulation of the R-point behavior (here defined as the minimum serum duration to enable E2F activation). The contribution of the positive feedback can be evaluated by changing α, which modulates the positive feedback strength. The contribution of the Myc input can be modulated by changing β. As shown in Supplementary Figure 6B and 6C, both the positive feedback and Myc input can significantly change the R-point. In particular, sufficiently strong Myc input can lead to a monostable system (eliminating R-point), and the R-point increases with decreasing Myc input. However, the system will still maintain an R-point even without the Myc input. Also, we note that the R-point is in fact highly sensitive to the strength of the positive feedback when the latter is weak (small α).

Supplementary References

1. Johnson, D.G., Ohtani, K. & Nevins, J.R. Autoregulatory control of E2F1 expression in response to positive and negative regulators of cell cycle progression. *Genes & development* **8**, 1514-1525 (1994).
2. Morita, S., Kojima, T. & Kitamura, T. Plat-E: an efficient and stable system for transient packaging of retroviruses. *Gene therapy* **7**, 1063-1066 (2000).
3. Logan, J. *et al.* Transformation by adenovirus early region 2A temperature-sensitive mutants and their revertants. *Virology* **115**, 419-422 (1981).
4. Motokura, T. & Arnold, A. PRAD1/cyclin D1 proto-oncogene: genomic organization, 5' DNA sequence, and sequence of a tumor-specific rearrangement breakpoint. *Genes, chromosomes & cancer* **7**, 89-95 (1993).
5. Todorov, I.T., Attaran, A. & Kearsey, S.E. BM28, a human member of the MCM2-3-5 family, is displaced from chromatin during DNA replication. *The Journal of cell biology* **129**, 1433-1445 (1995).
6. You, L., Hoonlor, A. & Yin, J. Modeling biological systems using Dynetica--a simulator of dynamic networks. *Bioinformatics* **19**, 435-436 (2003).
7. Doedel, E.J. AUTO, a program for the automatic bifurcation analysis of autonomous systems. *Cong. Numer.* **30**, 265-384 (1981).
8. Ermentrout, B. Simulating, Analyzing, and Animating Dynamical Systems. *SIAM Press, Philadelphia* (2002).
9. Sears, R., Leone, G., DeGregori, J. & Nevins, J.R. Ras enhances Myc protein stability. *Molecular Cell* **3**, 169-179 (1999).
10. Sears, R. *et al.* Multiple Ras-dependent phosphorylation pathways regulate Myc protein stability. *Genes & Development* **14**, 2501-2514 (2000).
11. Yeh, E. *et al.* A signalling pathway controlling c-Myc degradation that impacts oncogenic transformation of human cells.[see comment]. *Nature Cell Biology* **6**, 308-318 (2004).
12. Helin, K. Regulation of cell proliferation by the E2F transcription factors. *Current Opinion in Genetics & Development* **8**, 28-35 (1998).
13. Diehl, J.A., Zindy, F. & Sherr, C.J. Inhibition of cyclin D1 phosphorylation on threonine-286 prevents its rapid degradation via the ubiquitin-proteasome pathway. *Genes & Development* **11**, 957-972 (1997).
14. Sherr, C.J. & Roberts, J.M. CDK inhibitors: positive and negative regulators of G1-phase progression. *Genes & Development* **13**, 1501-1512 (1999).

15. Clurman, B.E., Sheaff, R.J., Thress, K., Groudine, M. & Roberts, J.M. Turnover of cyclin E by the ubiquitin-proteasome pathway is regulated by cdk2 binding and cyclin phosphorylation. *Genes & Development* **10**, 1979-1990 (1996).
16. Won, K.A. & Reed, S.I. Activation of cyclin E/CDK2 is coupled to site-specific autophosphorylation and ubiquitin-dependent degradation of cyclin E. *EMBO Journal* **15**, 4182-4193 (1996).
17. Mihara, K. *et al.* Cell cycle-dependent regulation of phosphorylation of the human retinoblastoma gene product. *Science* **246**, 1300-1303 (1989).
18. Buchler, N.E., Gerland, U. & Hwa, T. Nonlinear protein degradation and the function of genetic circuits. *PNAS* **102**, 9559-9564 (2005).
19. Kholodenko, B.N. Cell-signalling dynamics in time and space. *Nature Reviews Molecular Cell Biology* **7**, 165-176 (2006).
20. Park, S. *et al.* Determination of binding constant of transcription factor myc-max/max-max and E-box DNA: the effect of inhibitors on the binding. *Biochimica et Biophysica Acta (BBA) - General Subjects* **1670**, 217-228 (2004).
21. Grafstrom, R.H., Pan, W. & Hoess, R.H. Defining the substrate specificity of cdk4 kinase-cyclin D1 complex. *Carcinogenesis* **20**, 193-198 (1999).
22. Pan, W., Sun, T., Hoess, R. & Grafstrom, R. Defining the minimal portion of the retinoblastoma protein that serves as an efficient substrate for cdk4 kinase/cyclin D1 complex. *Carcinogenesis* **19**, 765-769 (1998).